High Power Laser Science and Engineering, (2024), Vol. 12, e36, 8 pages.
doi:10.1017/hpl.2024.18

HIGH POWER LASER SCIENCE AND ENGINEERING

RESEARCH ARTICLE

New grating compressor designs for XCELS and SEL-100 PW projects

Efim Khazanov

Gaponov-Grekhov Institute of Applied Physics of the Russian Academy of Sciences, Niznij Novgorod, Russia

(Received 28 December 2023; revised 29 January 2024; accepted 25 March 2024)

Abstract

The problem of optimizing the parameters of a laser pulse compressor consisting of four identical diffraction gratings is solved analytically. The goal of optimization is to obtain maximum pulse power, completely excluding both beam clipping on gratings and the appearance of spurious diffraction orders. The analysis is carried out in a general form for an out-of-plane compressor. Two particular 'plane' cases attractive from a practical point of view are analyzed in more detail: a standard Treacy compressor (TC) and a compressor with an angle of incidence equal to the Littrow angle (LC). It is shown that in both cases the LC is superior to the TC. Specifically, for 160-cm diffraction gratings, optimal LC design enables 107 PW for XCELS and 111 PW for SEL-100 PW, while optimal TC design enables 86 PW for both projects.

Keywords: Littrow angle compressor; multi-petawatt lasers; Treacy compressor

1. Introduction

In 100-PW laser projects[1–9], where Nd:glass laser pulses with an energy of about 10 kJ are used for pumping, the output pulse energy is limited by the laser-induced damage threshold of the compressor diffraction gratings. The damage threshold of gratings by nanosecond pulses is much higher than by femtosecond ones[10]. Therefore, despite there being less energy incident on the last grating than on the first one, the laser damage threshold of the last grating is of major importance. Thus, the maximum output energy W is proportional to the squared beam size d, threshold value of fluence w_{th} (in the plane normal to the beam wave vector), reflection coefficient R of the grating and fill-factor η, taking into account fluence inhomogeneity in the beam:

$$W = R\eta w_{\text{th}} d^2. \tag{1}$$

Here, we assume that the beam has a square cross-section. Increasing w_{th} and R is a technological task that is beyond the scope of this paper. The fill-factor η depends on the energy and spectral properties of the spatial noise of the beam, in particular, on the root mean square (rms) and effective spatial frequency[11]. Both of these parameters can be significantly reduced by using an asymmetric compressor[5,12–14] or a compressor with an out-of-plane geometry[15]. The purpose of this work is to search for the following compressor parameters: angle of incidence on the first grating α, distance between the gratings along the normal L and groove density N that allow obtaining the maximum value of W. Bearing in mind that w_{th} does not depend on the angle of incidence α on the grating[16,17], we will assume that w_{th}, R and η are constants that do not depend on the compressor parameters. Thus, an optimal compressor design (α, L, N) is a design that ensures a maximum value of d^2. Note that in Equation (1), R is to the power of one rather than four, as laser-induced damage restrictions are important only for the last grating.

The main restriction on increasing d is the fact that on the second grating the beam size should not be larger than the grating length L_g. A standard compressor[18] consists of identical gratings, with the gratings of the first and second pairs being antiparallel to each other (see Figure 1(a)). We will further call such a compressor a Treacy compressor (TC). The TC is used in the vast majority of high-power lasers[19]. The maximization of d was considered in Ref. [20] in the $\omega_0 \gg \Omega$ approximation (ω_0 is the center frequency and Ω is the bandwidth). For pulses with a duration of less than 50 fs, this approximation is not accurate. However, in this case it can be readily shown that, for a given dispersion

Correspondence to: Efim Khazanov, Gaponov-Grekhov Institute of Applied Physics of the Russian Academy of Sciences, Niznij Novgorod 603950, Russia. Email: efimkhazanov@gmail.com

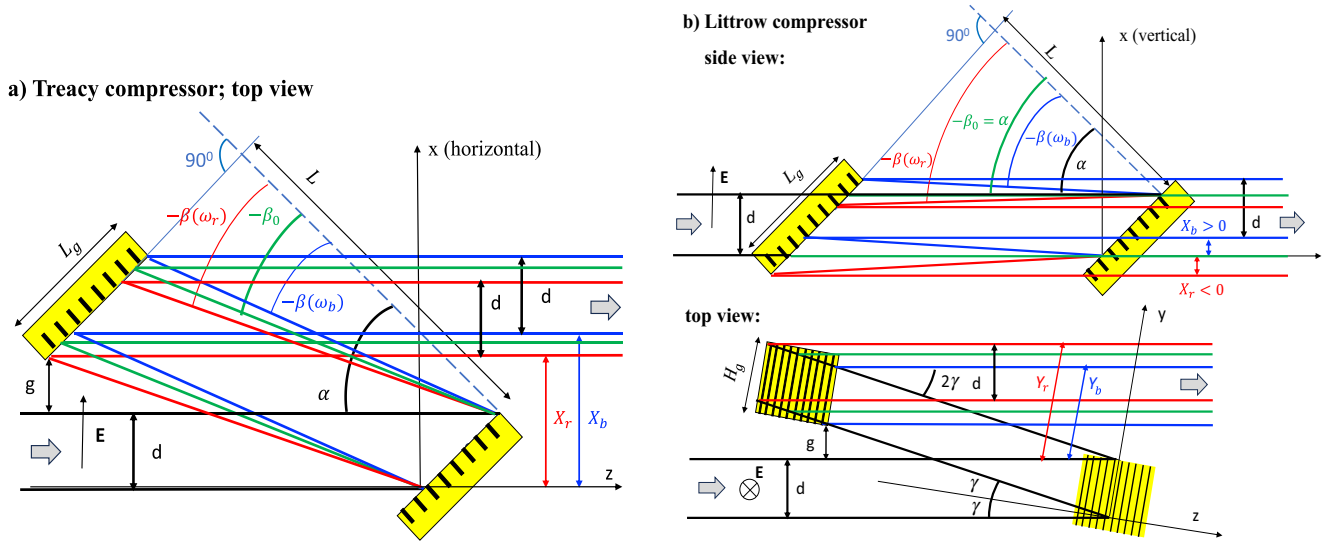

Figure 1. TC (a) and LC (b). The second half of the compressor (third and fourth gratings) is absolutely symmetric to the first one, so it is not shown in the figure. The angle of reflection in the diffraction plane is $\beta < 0$, which explains the minus sign in the figure. The angle of reflection in the plane orthogonal to the diffraction plane is always equal to the angle of incidence γ.

of a chirped pulse and given N, d is proportional to $\cos\alpha$. Then, from Equation (1) it can be found that for increasing W it is necessary to decrease α. However, the decrease in α makes decoupling impossible, that is, the condition that the second grating must not overlap with the input beam cannot be fulfilled. It is obvious that decoupling is impossible if $\alpha \approx \alpha_L$, where α_L is the Littrow angle. As will be shown below for a general case, that is, outside the $\omega_0 \gg \Omega$ approximation, at certain parameters an optimal compressor is a TC with $\alpha < \alpha_L$.

For $\alpha \approx \alpha_L$, decoupling may be provided employing an out-of-plane compressor[21] that is used, for example, for spectral beam combining[22] and for compressing narrow-beam pulses[23]. In this work we propose to use an out-of-plane compressor for increasing output power by decreasing α down to $\alpha = \alpha_L$ and $\alpha < \alpha_L$, inclusive. Both multilayer dielectric[24] and gold gratings[16,24] in the out-of-plane geometry may have a reflection coefficient R almost the same as in the out-of-plane geometry. It is important to note that for $\alpha = \alpha_L$ the out-of-plane compressor 'turns out' to be plane again (Figure 1(b)), which greatly simplifies its experimental implementation. Such a compressor will be referred to as a compressor with an angle of incidence equal to the Littrow angle (LC). The LC has a number of additional advantages[24], one of which is the use of multilayer dielectric gratings, the reflection band of which rapidly narrows with increasing $\alpha - \alpha_L$, which makes them unfit for the TC in wideband lasers[25]. An important issue of radiation polarization in the out-of-plane compressor was discussed in detail in Ref. [24].

Analytical expressions that allow for finding the compressor parameters that provide maximum values of d for both the TC and LC will be obtained in Section 2. Optimal designs of both compressors for the XCELS project[4] will be discussed in detail in Section 3. An analogous optimization for the pulse parameters of the SEL-100 PW project[1,3,10] will be made in Section 4.

2. Maximum beam size for the TC and the LC

We will first consider a general case of an out-of-plane compressor when the angles of incidence on the first grating in two planes γ and α are arbitrary. The TC (Figure 1(a)) and LC (Figure 1(b)) are its particular cases at $\gamma = 0$ and $\alpha = \alpha_L$, respectively. Note that, both in the TC and LC, the gratings of the first and second pairs are antiparallel (mirror) to each other in the planes orthogonal to the incident beam. The case of non-parallel gratings is considered, for example, in Ref. [26]. The maximum beam size will be determined using the following procedure. We choose the coordinate system (x, y, z) as shown in Figure 1: the y-axis is parallel to the direction of the grooves, and the x-axis in the (x, z) diffraction plane is directed at an angle α to the surface of the grating. The coordinate origin coincides with the point of incidence of the beam on the first grating. Let us find the spectral phase $\Psi(\omega, k_x, k_y)$ accumulated in the beam on reflection from the first grating, propagation to the second grating, reflection from the second grating and propagation to the $z = 0$ plane. The first derivatives of Ψ with respect to k_x, k_y up to the sign are equal to the beam coordinates $X(\omega)$ and $Y(\omega)$ in the $z = 0$ plane. These coordinates will allow, for geometric reasons, one to determine the maximum beam size d depending on the parameters of the compressor and the input pulse. The expression for Ψ is available in Refs. [18, 27]; in the chosen coordinate system it has the

https://doi.org/10.1017/hpl.2024.18 Published online by Cambridge University Press

following form:

$$\Psi\left(\omega,k_x,k_y\right)=Lk_{zx}\left(\cos\theta+\cos\left(\alpha+\operatorname{atan}\frac{k_x}{k_z}\right)\right),\qquad(2)$$

where $k_{zx}^2=\frac{\omega^2}{c^2}-k_y^2$, $k_z^2=\frac{\omega^2}{c^2}-k_x^2-k_y^2$ and θ is the angle of reflection from the grating:

$$\sin\theta\left(\omega,k_x,k_y\right)=-\frac{2\pi}{k_{zx}}N+\sin\left(\alpha+\operatorname{atan}\frac{k_x}{k_z}\right).\qquad(3)$$

Hereinafter, we assume the minus first diffraction order. In the chosen reference frame, the transverse wave vectors are related to the incidence angles α and γ as $k_x=0$, $k_y=\frac{\omega}{c}\sin\gamma$. Taking into account the large beam size we neglect diffraction, that is, the second derivatives of Ψ with respect to k_x,k_y. Then, upon differentiation of Equation (2) with allowance for Equation (3) we find the derivatives of interest to us:

$$\Psi'_{k_x}\left(\omega,k_x=0,k_y=\frac{\omega}{c}\sin\gamma\right)=-X\left(\omega\right)=-L\frac{\sin\left(\beta+\alpha\right)}{\cos\beta},\qquad(4)$$

$$\Psi'_{k_y}\left(\omega,k_x=0,k_y=\frac{\omega}{c}\sin\gamma\right)=-Y\left(\omega\right)=-L\tan\gamma\frac{1+\cos\left(\beta+\alpha\right)}{\cos\beta},\qquad(5)$$

$$\frac{1}{2}\Psi''_{\omega\omega}\left(\omega=\omega_0,k_x=0,k_y=\frac{\omega}{c}\sin\gamma\right)=\mathrm{GVD}=-\frac{L}{\omega_0 c}\cos\gamma\frac{\left(\sin\alpha-\sin\beta_0\right)^2}{2\cos^3\beta_0},\qquad(6)$$

where the angle of reflection $\beta=\beta\left(\omega\right)$ is found from the following:

$$\sin\beta=-\frac{2\pi c}{\omega}\frac{N}{\cos\gamma}+\sin\alpha,\qquad(7)$$

and $\beta_0=\beta\left(\omega_0\right)$. The expression for GVD (Equation (6)) is derived in Ref. [21], and Equation (7) can be found in Refs. [22, 28]. The expression for GVD (Equation (6)) with allowance for Equation (7) is the same as for GVD for the TC but with the substitution $L\to L\cos\gamma;N\to N/\cos\gamma$. From Equations (2) and (3) it can be readily shown that this remark is true for all frequency derivatives, that is, for all dispersion orders. This circumstance can be used for high-order dispersion management of the entire laser system, including the stretcher, acousto-optics spectral phase control and compressor.

We will consider only the case when the beam is not clipped on the second grating (the case of clipping has been considered in detail in a number of works, e.g., Refs. [3, 5, 12, 29, 30], and will be briefly discussed in Section 4), so we will assume straight away that the beam size on the second grating coincides with its length L_g and height H_g. Taking this into account, from Figure 1 the following can be found:

$$L_\mathrm{g}=\frac{d+\mid X_\mathrm{b}-X_\mathrm{r}\mid\cos\gamma}{\cos\alpha},\qquad(8)$$

$$H_\mathrm{g}=\frac{d+\left|Y_\mathrm{b}-Y_\mathrm{r}\right|\cos\gamma}{\cos\gamma}+\left(d-\left|X_\mathrm{b}-X_\mathrm{r}\right|\right)\tan\gamma\tan\alpha,\qquad(9)$$

where $X_\mathrm{b}=X\left(\omega_\mathrm{b}\right),X_\mathrm{r}=X\left(\omega_\mathrm{r}\right)$, $Y_\mathrm{b}=Y\left(\omega_\mathrm{b}\right)$, $Y_\mathrm{r}=Y\left(\omega_\mathrm{r}\right)$ and $\omega_{\mathrm{b,r}}$ are the high-frequency and low-frequency boundaries of the pulse spectrum. When deriving Equations (8) and (9), we took into account that $X_{\mathrm{b,r}}$ and $Y_{\mathrm{b,r}}$ are the beam coordinates in the plane perpendicular to the z-axis, but not in the plane normal to the beam, and also that the gratings are tilted in two planes (the second term in Equation (9)). From Equations (8) and (9) with allowance for Equations (4)–(6) we obtain the following:

$$L_\mathrm{g}=\frac{d}{\cos\alpha}+L_\mathrm{disp}\frac{1}{\cos\gamma}\frac{2\cos^3\beta_0}{\left(\sin\alpha-\sin\beta_0\right)^2}\left|\operatorname{atan}\beta_\mathrm{b}-\operatorname{atan}\beta_\mathrm{r}\right|,\qquad(10)$$

$$H_\mathrm{g}=d\left(\frac{1+\tan\alpha\sin\gamma}{\cos\gamma}\right)+L_\mathrm{disp}\frac{2\cos^3\beta_0\left|\tan\gamma\right|}{\left(\sin\alpha-\sin\beta_0\right)^2}\times\left(\frac{1}{\cos\gamma}\left|\frac{1+\cos\left(\beta_\mathrm{b}+\alpha\right)}{\cos\beta_\mathrm{b}}-\frac{1+\cos\left(\beta_\mathrm{r}+\alpha\right)}{\cos\beta_\mathrm{r}}\right|-\sin\alpha\left|\operatorname{atan}\beta_\mathrm{b}-\operatorname{atan}\beta_\mathrm{r}\right|\right),\qquad(11)$$

where $L_\mathrm{disp}=\mid\mathrm{GVD}\mid\omega_0 c$ and $\beta_\mathrm{b}=\beta\left(\omega_\mathrm{b}\right),\beta_\mathrm{r}=\beta\left(\omega_\mathrm{r}\right)$. The absence of beam clipping along the x-coordinate leads to limitations on the beam size d, which follows from Equation (10):

$$d<d_\mathrm{g}=\left(L_\mathrm{g}-L_\mathrm{disp}\frac{1}{\cos\gamma}\frac{2\cos^3\beta_0}{\left(\sin\alpha-\sin\beta_0\right)^2}\left|\tan\beta_\mathrm{b}-\tan\beta_\mathrm{r}\right|\right)\cos\alpha.\qquad(12)$$

This expression is identical for the TC and LC. In the $\omega_0\gg\Omega$ approximation, Equation (12) transforms to the expression obtained in Ref. [20] under this approximation. The second limitation on d is the need to ensure decoupling of the beams, that is, non-overlapping of the second grating with the incident beam. For the TC, decoupling is attained in the direction of the x-axis (Figure 1(a)). Obviously, for this the minimum beam displacement $\mid X_\mathrm{min}\mid$ should be larger than the beam size d plus the minimum required technological gap g:

$$\mid X_\mathrm{min}\mid>d+g.\qquad(13)$$

For $\alpha>\alpha_\mathrm{L}$ (the case in Figure 1(a)), $X_\mathrm{min}=X_\mathrm{r}$, and for $\alpha<\alpha_\mathrm{L}$, vice versa, $X_\mathrm{min}=X_\mathrm{b}$. Taking this into account, from Equations (4) and (13) we obtain for the TC the following expression:

https://doi.org/10.1017/hpl.2024.18 Published online by Cambridge University Press

$$d < d_{\mathrm{i}} = JL_{\mathrm{disp}} - g \quad \text{for the TC}, \tag{14}$$

where

$$J = \begin{cases} \frac{\sin(\beta_{\mathrm{r}}+\alpha)}{\cos\beta_{\mathrm{r}}} \frac{2\cos^3\beta_0}{(\sin\alpha-\sin\beta_0)^2} & \text{for } \alpha > \alpha_{\mathrm{L}} \\ \frac{|\sin(\beta_{\mathrm{b}}+\alpha)|}{\cos\beta_{\mathrm{b}}} \frac{2\cos^3\beta_0}{(\sin\alpha-\sin\beta_0)^2} & \text{for } \alpha < \alpha_{\mathrm{L}} \end{cases}. \tag{15}$$

The expression analogous to Equation (14) was presented in Ref. [20] in different notation. For the LC, decoupling occurs in the direction of the y-axis and requires that the minimum beam displacement $|\, Y_{\min} \,| \cos\gamma$ should be larger than $d+g$. Since the gratings are tilted in two planes, then strictly speaking, g is a function of the angles α and γ, but further for simplicity we will assume $g = \text{const}$. The most stringent condition for decoupling is for frequency ω_{b}: $|\, Y_{\mathrm{b}} \,| \cos\gamma > d+g$. With this taken into account, from Equation (5) we obtain the following:

$$d < d_{\mathrm{i}} = IL_{\mathrm{disp}} - g \ \text{ for the LC}, \tag{16}$$

where

$$I = |\tan\gamma| \frac{1+\cos(\beta_{\mathrm{b}}+\alpha)}{\cos\beta_{\mathrm{b}}} \frac{2\cos^3\beta_0}{(\sin\alpha-\sin\beta_0)^2}. \tag{17}$$

In addition to meeting the conditions in Equations (12), (14) and (16), it is essential that there are no diffraction orders other than the minus first one. This condition is always more stringent for radiation with frequency ω_{b}. Let us introduce the function $\Pi(\alpha)$, which is equal to zero if at least one of these diffraction orders is as follows:

$$\Pi(\alpha) = \begin{cases} 0 & \text{if} \quad \sin\alpha < 1 - \frac{2\pi c}{\omega_{\mathrm{b}}} \frac{N}{\cos\gamma} \text{ or } \sin\alpha > \frac{4\pi c}{\omega_{\mathrm{b}}} \frac{N}{\cos\gamma} - 1 \\ 1 & \text{if} \quad \text{otherwise} \end{cases}. \tag{18}$$

The two conditions on the top line correspond to the first and minus second order of diffraction, respectively. Thus, the maximum beam size D, determined by simultaneous fulfillment of the three above conditions, has the following form:

$$D = \min\left\{d_{\mathrm{g}}; d_{\mathrm{i}}\right\} \Pi(\alpha), \tag{19}$$

where d_{g} and $\Pi(\alpha)$ are found from Equations (12) and (18) for both compressors, and d_i from Equation (14) for the TC and from Equation (16) for the LC. Note that the above expressions for the LC are valid for any out-of-plane compressor, that is, for any angle α, as we have not used the condition $\alpha = \alpha_{\mathrm{L}}$ when deriving these expressions.

It is convenient to conduct further discussion on the example of specific parameters of a compressed pulse, which will be addressed in the next two sections. Here, for reference we provide useful formulas for L and α_{L} that follow from Equations (6) and (7):

$$L = |\mathrm{GVD}|\, \omega_0 c \frac{1}{\cos\gamma} \frac{2\cos^3\beta_0}{(\sin\alpha-\sin\beta_0)^2}, \tag{20}$$

$$\sin\alpha_{\mathrm{L}} = \frac{\pi c}{\omega_0} \frac{N}{\cos\gamma}. \tag{21}$$

3. Optimization of the TC and the LC for the XCELS project

Let us consider the parameters for the XCELS project[4]: $L_{\mathrm{g}} = 138$ cm, $\lambda_0 = 910$ nm, $\Delta\lambda = 150$ nm, $g = 2$ cm and $2\mathrm{GVD} = -4.4$ ps^2. Here, 2GVD is the dispersion of two grating pairs, that is, like above, GVD is the dispersion of one grating pair. As an example, the dependence of a number of parameters on α for $N = 1050$/mm is plotted in Figure 2. The yellow line shows the Littrow angle for clarity. The green curve d_{g} in Equation (12) corresponds to the restrictions on the beam size imposed by the condition of the absence of beam clipping. The blue curve d_{i} corresponds to the restrictions on the beam size imposed by the need for decoupling in the diffraction plane for the TC (Equation (14); Figure 1(a)) and in the orthogonal plane for the out-of-plane compressor (Equation (16); Figure 1(b)). The black square wave shows the range of angles in which there are no other diffraction orders (Equation (18)): the first order is possible to the left of the square wave, and the minus second order to the right. Finally, the red dashed curve combines the three above restrictions for the $D(\alpha)$ relation (Equation (19)). The maximum value of this curve corresponds to the maximum beam size (at $N = 1050$/mm) and, therefore, the maximum output energy and pulse power after the compressor. The behavior of the curve $D(\alpha)$ greatly depends on N for both the TC and LC (Figure 3). The curves in Figure 3(a) (for the TC) have two local maxima. At large N the global maximum is at $\alpha > \alpha_{\mathrm{L}}$, and at small N is at $\alpha < \alpha_{\mathrm{L}}$.

The parameters of an out-of-plane compressor can be optimized in a wide range of angles α, including $\alpha < \alpha_{\mathrm{L}}$. All of the above expressions are valid for any α. In what will follow we will restrict consideration to the case of the LC ($\alpha = \alpha_{\mathrm{L}}$, Figure 1(b)), which is interesting from the practical point of view. Recently, the possibility of developing gratings having length $L_{\mathrm{g}} = 160$ cm and the parameters of a compressor with such gratings have been discussed in the literature[5,16]. Here, we will find parameters of the optimal compressor for XCELS for two options: $L_{\mathrm{g}} = 138$ cm and $L_{\mathrm{g}} = 160$ cm.

The maximum size of the beam D, both in the LC and TC, depends on two parameters: N and α for the TC and N and γ for the LC. For each N there exists an optimal value of the angle α_{opt} or γ_{opt} at which D is the maximum.

https://doi.org/10.1017/hpl.2024.18 Published online by Cambridge University Press

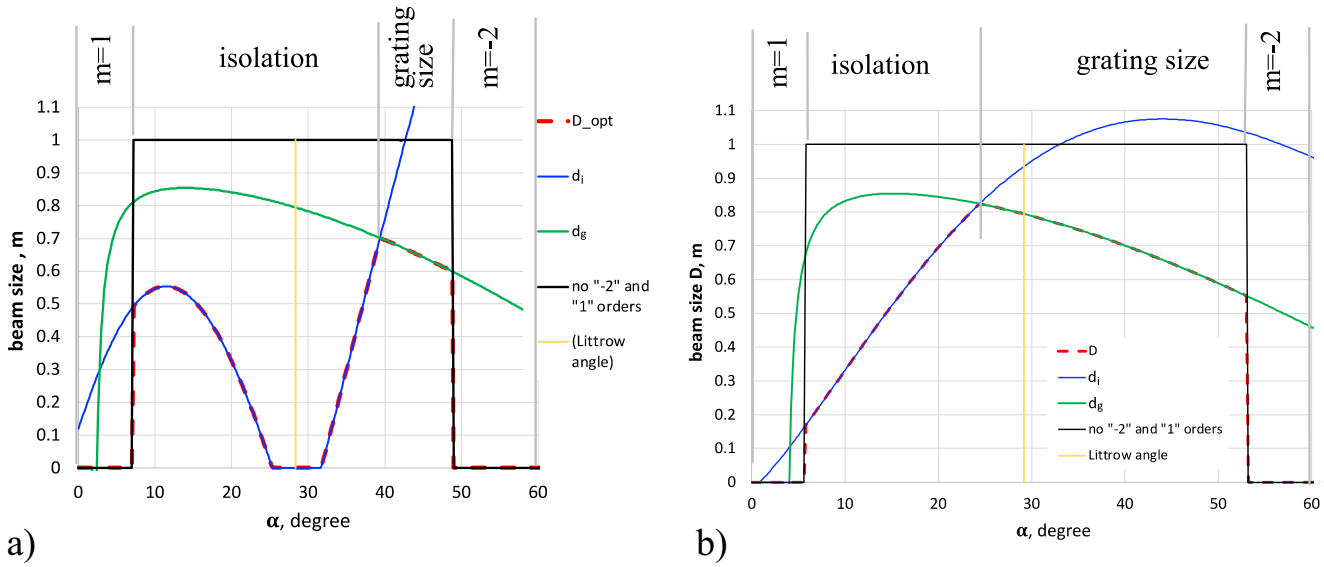

Figure 2. Restrictions on maximum beam size at $L_g = 138$ cm, $N = 1050$/mm for the TC (a) and for the out-of-plane compressor at $\gamma = 13°$ (b). Green curve for d_g (Equation (12)) – no beam clipping on the grating; blue curve for d_i (Equations (14) and (16)) – decoupling needed; black square wave $\Pi(\alpha)$ (Equation (18)) – range of angles without other diffraction orders (Equation (18)), the first order is possible to the left of the square wave and the minus second order to the right; the red dashed curve combines all restrictions and shows $D(\alpha)$ (Equation (19)); the yellow line shows the Littrow angle for clarity.

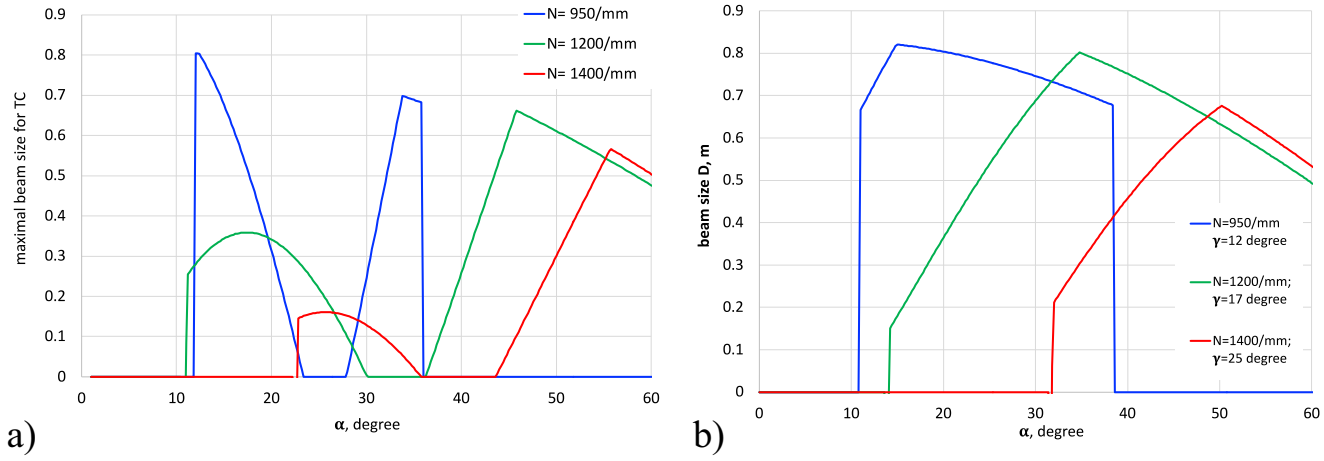

Figure 3. Maximum beam size $D(\alpha)$ for the TC (a) and for the out-of-plane compressor (b) for $L_g = 138$ cm and $N = 950$/mm (blue), $N = 1200$/mm (green) and $N = 1400$/mm (red).

The relations $D_{opt}(N) = D(N, \alpha_{opt})$ for the TC and $D_{opt}(N) = D(N, \gamma_{opt})$ for the LC are shown in Figures 4(a) and 4(b) by triangles for $L_g = 138$ cm and by squares for $L_g = 160$ cm. For $L_g = 138$ cm, the maximum value of the beam size D_m is the same for the LC and TC. For the TC, $D_{opt}(N)$ has a well-pronounced maximum at $N = 950$/mm, whereas for the LC, conversely, it has a plateau in the N range of 1000/mm to 1250/mm. This is an advantage of the LC, since it gives freedom to choose N. The choice of a specific value of N may be made, for example, for reasons of a higher efficiency, a higher laser-induced damage threshold of the grating, etc. Note that $D_m = 78$ cm is much larger than the beam diameter in the initial XCELS design (see Table 1). An analogous plateau in the N range of 950/mm to 1150/mm is observed in the $D_{opt}(N)$ function for the LC at $L_g = 160$ cm. In this case, the LC is obviously more preferable, since it enables a larger value of D_m: 96 cm versus 86 cm for the TC.

The circles and diamonds in Figure 4(a) correspond to the dependence of $\alpha - \alpha_L$ on N. It is clearly seen that for large N, $\alpha > \alpha_L$, which corresponds to a standard compressor design for high-power lasers. At the same time, for small N, the maximum beam size D_m is attained at $\alpha < \alpha_L$. This is also well seen in Figure 3(a) (left-hand maximum in the blue curve above the right-hand maximum). We are not aware of the usage of the TC with $\alpha < \alpha_L$ in high-power lasers. The circles and diamonds in Figure 4(b) show $\gamma(N)$ at which $\alpha = \alpha_L$. In the region of the $D_{opt}(N)$ plateau, that is, at $N = 950/\text{mm}$ to 1200/mm, $\gamma = 10° - 20°$, which falls within the range where the efficiency of the gratings almost does not decrease[16,24].

https://doi.org/10.1017/hpl.2024.18 Published online by Cambridge University Press

Table 1. Compressor parameters.

	XCELS $\lambda = (910 \pm 75)$ nm					SEL-100 PW $\lambda = (925 \pm 100)$ nm	
	$L_g = 138$ cm			$L_g = 160$ cm		$L_g = 160$ cm	
	TC[4]	TC (new)	LC	TC	LC	TC	LC
N, mm^{-1}	1200	950	1100	950	1000	1000	1100
α, degree	46.2	12.2	30.5	36.0	27.4	38.8	31.3
γ, degree	0	0	11.6	0	11.2	0	14.8
D_m, cm	66	78	78	86	96	75	85
H_g, cm	66	78	94	86	112	75	110
W^a, J	1006	1410	1410	1720	2130	1284	1670
τ, fs	20	20	20	20	20	15	15
P, PW	50	71	71	86	107	86	111

[a]Given that $R\eta w_{th} = 0.231$ J/cm^2 in the plane normal to the beam.

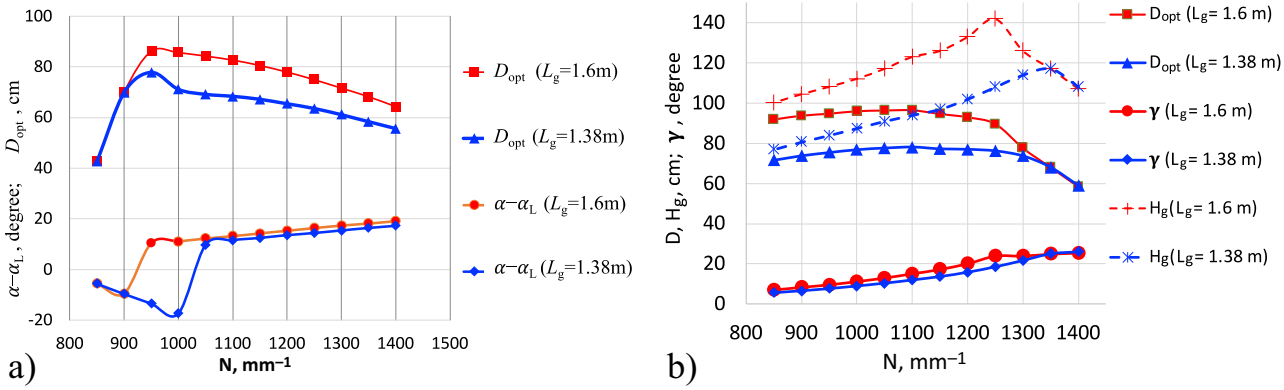

Figure 4. Curves for compressor parameters for XCELS for the TC (a) and the LC (b) with grating length $L_g = 138$ cm (blue) and $L_g = 160$ cm (red). Squares and triangles – beam size D_{opt} at optimal angles α and γ; circles and diamonds – difference between the incidence angle in the diffraction plane and the Littrow angle ($\alpha - \alpha_L$) (a) and the incidence angle in the plane orthogonal to the diffraction plane γ (b); plus signs and asterisks in (b) – grating height H_g.

It is worth noting the LC drawback: the grating height H_g is larger than the beam size. The dashed curves in Figure 4(b) show $H_g(N)$ plotted by Equation (11). At the same time, the increase in H_g required for the LC is not so great – compare the curves for $H_g(N)$ and $D_{opt}(N)$ – and may well be implemented in practice. In any case, 160-cm-long gratings have a height of about 100 cm, which is just a little bit smaller than the requirements for the LC for XCELS and SEL-100 PW (see Table 1). Still another LC drawback is that in a general case the choice of input beam polarization is nontrivial. This issue was studied in detail in Ref. [24]. From the analysis made in Ref. [24] it follows that vertical incident polarization, when the field is normal to the direction of the grooves, is optimal (Figure 1(b)). The experiment[24] carried out at $\gamma = 15°$ showed that in this case the reflection coefficient of one grating R and the efficiency of the entire compressor differ negligibly from the corresponding parameters at $\gamma = 0$. These results were obtained for a wavelength of 800 nm and $N = 1480$/mm; they need clarification for other wavelengths and groove densities.

The main parameters of the TC and LC for the XCELS project are presented in Table 1. For comparison of different designs, it also contains values of maximum beam energy W calculated by Equation (1), given that $R\eta w_{th} = 0.231$ J/cm^2, which corresponds to $R = 0.92$, and the value of safe fluence $\eta w_{th} = 0.251$ J/cm^2 in the plane normal to the beam, that is, 0.174 J/cm^2 on the grating surface at $\alpha = 46°$[4]. Note that this is a rather conservative estimate, since gratings with $w_{th} = 0.4$ J/cm^2 and $w_{th} = 0.57$ J/cm^2 in the plane normal to the beam are reported in Refs. [16] and [31], and $\eta = 1.31$[4,10] or $\eta = 1.41$[5] are considered in the literature for η. The Fourier-transform-limited pulse in XCELS has a duration of 17 fs, whereas the values of maximum power in Table 1 are given for a 20 fs pulse, which is more realistic in practice. It is clear from the table that the new TC and LC designs with a grating length of 138 cm allow for increasing the output power by a factor of 1.42, that is, up to 71 PW. With the use of 160 cm × 112 cm gratings in the LC, over 100 PW may be achieved.

4. The TC and the LC for SEL-100 PW

Let us consider the parameters for the SEL-100 PW project[1,3,10,32]: $L_g = 160$ cm, 2GVD = –4.2 ps^2, $\lambda_0 = 925$ nm, $\Delta\lambda = 200$ nm and $g = 2$ cm. For these values, the optimal parameters for the TC and LC are listed in

https://doi.org/10.1017/hpl.2024.18 Published online by Cambridge University Press

Table 1. Since the pulse spectrum width in the SEL-100 PW is 1.33 times larger than that in XCELS, for a correct comparison we assume the 15-fs pulse duration to be 1.33 times shorter than in XCELS. It is seen from the table that, for a grating size of 160 cm × 75 cm, the optimal design of the TC provides an output power of 86 PW. In this case, the angle of incidence α differs from the Littrow angle only by 11.5°. The LC allows for achieving a significantly higher power of 111 PW with 160 cm × 110 cm gratings. The angle γ, in this case, despite being larger than in the other designs presented in Table 1, still falls within the range in which the grating efficiency almost does not reduce[16,24].

It is important to note that the analysis made in this work completely excludes beam clipping by gratings. The design of the two-grating compressor for the SEL-100 PW presented in Ref. [5] implies strong clipping. This leads to three effects that reduce the focal intensity: pulse stretching due to narrowing of the spectrum; loss of radiation energy; and deterioration of focusability. In the example numerically calculated in Ref. [5], the losses were approximately 11%, 7.8% and 15%, that is, more than 35% in total. It is worthy to note that these losses cannot be compensated by increasing the pulse energy at the compressor input, as clipping does not reduce fluence on the last grating. Therefore, according to Equation (1) the compressor[5] enables 35% lower focal intensity than a compressor without clipping for the same values of w_{th}, R, η and d.

Comparison of the compressor parameters for XCELS and SEL-100 PW with 160-cm long gratings shows that for the TC the maximum achievable power is the same – 86 PW; whereas for the LC the SEL-100 PW power is 4% higher – 111 PW versus 107 PW. However, from a practical point of view, the XCELS option is preferable, since for a narrower pulse spectrum, the requirements for both the compressor gratings and the rest of the optics are lower. At the same time, XCELS requires 1.33 times higher pulse energy; hence, deuterated potassium dihydrogen phosphate (DKDP) crystals with $\sqrt{1.33} = 1.15$ times larger size are required.

All spatio-temporal phenomena in the out-of-plane compressor are the same as in the TC if the compressors are symmetric: $L_2 = L_1; N_2 = N_1; \alpha_2 = \alpha_1; \gamma_2 = \gamma_1$, where the indices '1' and '2' correspond to the first and second grating pairs, respectively. All the compressor variants discussed above are symmetric. At the same time, they can be easily modified into asymmetric compressors that ensure reduction of fluence fluctuations due to the time delay of high-frequency spatial harmonics[13,15] or spatial dispersion of the output beam[5,12,14]. In asymmetric compressors, grating pairs differ from each other: $L_2 \neq L_1$[5,12,14]; $N_2 \neq N_1$, $\alpha_2 \neq \alpha_1$[13]; $\gamma_2 \neq \gamma_1$[15]. Note that γ_2 and γ_1 can have not only different absolute values, but also signs. For example, for an LC with $\gamma_2 = -\gamma_1$, in which gratings of the first and second pairs are parallel in the y-plane and antiparallel (mirror) in the x-plane, they are two times shorter and two times wider than for the case $\gamma_2 = \gamma_1$. For $\gamma_1 \approx 10°$, fluence fluctuations are radically suppressed. The drawback of such a compressor is an additional increase in the grating height H_g.

5. Conclusion

Since in high-power femtosecond lasers the output pulse energy is limited by the laser-induced damage threshold of the last diffraction grating of the compressor, the optimal compressor design is the one ensuring maximum size of the output beam. For given parameters of a chirped pulse (central frequency, bandwidth, GVD) and a given diffraction grating length L_g, an analytical expression has been obtained for the maximum beam size D, at which both the beam clipping on the gratings and the appearance of spurious diffraction orders are completely excluded. Using this expression, it is easy to find the optimal compressor parameters that allow for obtaining maximum D: the distance between the gratings along the normal L, the groove density N, the angle of incidence on the first grating in the diffraction plane α and the angle of incidence on the first grating outside the diffraction plane γ.

The analysis was performed in a general form for an out-of-plane compressor, that is, for arbitrary values of the angles α and γ. Two particular 'plane' cases attractive for practical reasons were considered: a standard TC ($\gamma = 0$, Figure 1(a)) and an LC ($\alpha = \alpha_L$, Figure 1(b)). The LC almost always ensures a larger value of D than the TC. For the TC, $D(N)$ has a well-pronounced maximum determining the choice of N (Figure 4(a)). For the LC, $D(N)$ has the form of a plateau (Figure 4(b)), which allows for choosing N within this plateau for technological reasons: the larger the reflection coefficient, the higher the laser damage threshold.

Optimal TC and LC designs that enable a substantial output power increase (by tens of percent) were calculated for the pulse parameters of the XCELS and SEL-100 PW projects. In particular, for 160-cm-long diffraction gratings, the optimal TC design allows for obtaining 86 PW for both projects, and for the optimal LC design 107 and 111 PW for XCELS and SEL-100 PW, respectively.

Acknowledgements

The work was supported by the Ministry of Science and Higher Education of the Russian Federation (075-15-2020-906, Center of Excellence 'Center of Photonics'). The author thanks Anton Vyatkin and Ivan Yakovlev for fruitful discussions.

References

1. Y. Peng, Y. Xu, and L. Yu, Reza Kenkyu **49**, 93 (2021).
2. X. Wang, X. Liu, X. Lu, J. Chen, Y. Long, W. Li, H. Chen, X. Chen, P. Bai, Y. Li, Y. Peng, Y. Liu, F. Wu, C. Wang, Z. Li, Y.

https://doi.org/10.1017/hpl.2024.18 Published online by Cambridge University Press

Xu, X. Liang, Y. Leng, and R. Li, Ultrafast Sci. **2022**, 9894358 (2022).
3. Z. Li, J. Liu, Y. Xu, Y. Leng, and R. Li, Opt. Express **30**, 41296 (2022).
4. E. Khazanov, A. Shaykin, I. Kostyukov, V. Ginzburg, I. Mukhin, I. Yakovlev, A. Soloviev, I. Kuznetsov, S. Mironov, A. Korzhimanov, D. Bulanov, I. Shaikin, A. Kochetkov, A. Kuzmin, M. Martyanov, V. Lozhkarev, M. Starodubtsev, A. Litvak, and A. Sergeev, High Power Laser Sci. Eng. **11**, e78 (2023).
5. S. Du, X. Shen, W. Liang, P. Wang, J. Liu, and R. Li, High Power Laser Sci. Eng. **11**, e4 (2023).
6. Z. Li and J. Kawanaka, Rev. Laser Eng. **49**, 101 (2021).
7. Z. Li and J. Kawanaka, OSA Continuum **2**, 1125 (2019).
8. Z. Li, Y. Kato, and J. Kawanaka, Sci. Rep. **11**, 151 (2021).
9. J. Kawanaka, K. Tsubakimoto, H. Yoshida, K. Fujioka, Y. Fujimoto, S. Tokita, T. Jitsuno, N. Miyanaga, and Gekko-EXA Design Team , J. Phys. Conf. Ser. **688**, 012044 (2016).
10. J. Liu, X. Shen, S. Du, and R. Li, Opt. Express **29**, 17140 (2021).
11. A. Kochetkov, E. Kocharovskaya, and E. Khazanov, J. Opt. Soc. Am. B **40**, 2851 (2023).
12. X. Shen, S. Du, W. Liang, P. Wang, J. Liu, and R. Li, Appl. Phys. B **128**, 159 (2022).
13. E. Khazanov, High Power Laser Sci. Eng. **11**, e93 (2023).
14. X. Yang, X. Tang, Y. Liu, J. Bin, and Y. Leng, Opt. Express **31**, 33753 (2023).
15. E. Khazanov, Laser Phys. Lett. **20**, 125001 (2023).
16. Y. Han, Z. Li, Y. Zhang, F. Kong, H. Cao, Y. Jin, Y. Leng, R. Li, and J. Shao, Nat. Commun. **14**, 3632 (2022).
17. Y. Han, F. Kong, H. Cao, Y. Jin, and J. Shao, Proc. SPIE **12982**, 1298202 (2023).
18. E. B. Treacy, IEEE J. Quantum Electron. **QE-5**, 454 (1969).
19. I. V. Yakovlev, Quantum Electron. **44**, 393 (2014).
20. V. V. Romanov and K. B. Yushkov, IEEE J. Select. Top. Quantum Electron. **25**, 8800110 (2019).
21. K. Osvay and I. N. Ross, Opt. Commun. **105**, 271 (1994).
22. K. Wei and L. Li, Opt. Lett. **46**, 4626 (2021).
23. Š. Vyhlídka, P. Trojek, D. Kramer, D. Peceli, F. Batysta, J. Bartoníček, J. Hubáček, T. Borger, R. Antipenkov, E. Gaul, T. Ditmire, and B. Rus, Proc. SPIE **11034**, 1103409 (2019).
24. D. L. Smith, S. L. Erdogan, and T. Erdogan, Appl. Opt. **62**, 3357 (2023).
25. C. M. Werle, C. Braun, T. Eichner, T. Hulsenbusch, G. Palmer, and A. R. Maier, Opt. Express **31**, 37437 (2023).
26. J.-C. Chanteloup, E. Salmon, C. Sauteret, A. Migus, P. Zeitoun, A. Klisnick, A. Carillon, S. P. Hubert, D. Ros, P. Nickles, and M. Kalachnikov, J. Opt. Soc. Am. B **17**, 151 (2000).
27. J. J. Huang, L. Y. Zhang, and Y. Q. Yang, Opt. Express **19**, 814 (2011).
28. G. Kalinchenko, S. Vyhlidka, D. Kramer, A. Lererc, and B. Rus, Proc. SPIE **9626**, 96261R (2023).
29. B. C. Li, W. Theobald, E. Welsch, and R. Sauerbrey, Appl. Phys. B **71**, 819 (2000).
30. M. Trentelman, I. N. Ross, and C. N. Danson, Appl. Opt. **36**, 8567 (1997).
31. Y. Han, Y. Jin, F. Kong, Y. Wang, Y. Zhang, H. Cao, Y. Cui, and J. Shao, Appl. Surface Sci. **576**, 151819 (2022).
32. C. Wang, D. Wang, Y. Xu, and Y. Leng, Opt. Commun. **507**, 127613 (2022).

https://doi.org/10.1017/hpl.2024.18 Published online by Cambridge University Press